

Efficacy of Hsp90 inhibition for induction of apoptosis and inhibition of growth in cervical carcinoma cells in vitro and in vivo

Jörg Schwock · Nhu-An Pham · Mary P. Cao · David W. Hedley

Received: 18 December 2006 / Accepted: 7 May 2007 / Published online: 20 June 2007
© Springer-Verlag 2007

Abstract

Purpose Heat shock protein 90 (Hsp90) is a conserved chaperone involved in crucial signaling events in normal and malignant cells. Previous research suggests that tumor cells are particularly dependent on Hsp90 for survival as well as malignant progression. Hsp90 inhibitors which are derivatives of the natural compound geldanamycin, such as the orally bioavailable 17-(dimethylaminoethylamino)-17-demethoxygeldanamycin (17-DMAG), are currently being tested in clinical trials and small molecule inhibitors are in development. In this study we investigated the response of a panel of cervical carcinoma cell lines in vitro and in vivo to determine potential factors that might influence the sensitivity towards Hsp90 inhibition.

Methods Cell viability, proliferation and drug-induced changes on Hsp90 chaperoned “client” factors were examined with focus on G2/M cell cycle regulators, and a comparison with immortalized and normal keratinocytes was performed. ME180 and CaSki cells were grown as

subcutaneous xenografts in mice treated with 6–10 mg/kg 17-DMAG by oral gavage 2×/day on a chronic schedule. Tissue concentrations of 17-DMAG were measured by high performance liquid chromatography.

Results Cell death during abnormal mitosis was observed within 48 h after treatment start. ME180 and CaSki showed more cell death at this time point than SiHa and HeLa, and higher levels of pre-treatment Akt activity. IC₅₀ values ranged between 17 and 37 nM geldanamycin (MTS). Keratinocytes were at least as sensitive as carcinoma cells. All cell lines responded with an increase of the G2/M fraction. Despite in vitro effectiveness and tissue concentrations of 1 μM, only a limited tumor growth reduction was observed with 17-DMAG given close to the maximum tolerated dose level. Lower levels of Hsp90 protein, a lower Akt activity and signs of tissue hypoxia were observed in xenografts compared to cell cultures.

Conclusions We show here that Hsp90 inhibition effectively induces apoptosis and growth arrest in cervical carcinoma cells in vitro. Mitotic catastrophe was identified as one mechanism of cell death. In contrast, a limited efficacy of 17-DMAG was observed in subcutaneous xenograft models. Induction of a heat shock response has previously been implicated in resistance towards Hsp90 inhibition. Additional factors might be (1) an altered abundance and/or activity of primary (Hsp90) and secondary (e.g., Akt) target(s), (2) a narrow therapeutic range of 17-DMAG by oral application and (3) response-modifying factors within the tumor environment. The further development of synthetic Hsp90 inhibitors with increased therapeutic window is warranted.

J. Schwock · D. W. Hedley
Department of Laboratory Medicine and Pathobiology,
University of Toronto, 610 University Ave., 5th Floor,
Rm 203, M5G 2M9 Toronto, ON, Canada

N.-A. Pham · D. W. Hedley
Department of Medical Biophysics, University of Toronto,
610 University Ave., 5th Floor, Rm 203,
M5G 2M9 Toronto, ON, Canada

M. P. Cao · D. W. Hedley (✉)
Division of Applied Molecular Oncology, Princess Margaret
Hospital, Ontario Cancer Institute, University of Toronto,
610 University Ave., 5th Floor, Rm 203,
M5G 2M9 Toronto, ON, Canada
e-mail: david.hedley@uhn.on.ca

Keywords Hsp90 · Geldanamycin · Ansamycin · Pharmacodynamics · Xenograft

Introduction

Heat shock protein 90 (Hsp90) is a conserved and essential chaperone protein involved in the regulation of diverse biological processes such as cell signaling, proliferation and survival. The function of Hsp90 is to maintain the properly folded conformation of approximately 100 different “client” proteins, and inhibition of the chaperone results in the degradation of its clients by the proteasome. The biologically active form of Hsp90 has been identified as part of a multichaperone complex [1], and the preponderance of this form in tumor cells has been proposed as the rationale for Hsp90 targeted therapies [2].

Geldanamycin, isolated from *Streptomyces hygroscopicus* var. *geldanus*, was identified as the first Hsp90 inhibitor [3, 4], and its relatively specific inhibition was later recognized to be due to a structurally unique “Bergerat fold” ATP-binding site in Hsp90 [5]. Semi-synthetic benzoquinone ansamycin compounds developed based on the prototypic molecule include the 17-(allylamino)-17-demethoxygeldanamycin (17-AAG) and the water soluble 17-(dimethylaminoethylamino)-17-demethoxygeldanamycin (17-DMAG). These drug-like molecules are now being investigated in clinical trials [6]. 17-DMAG is more water soluble and shows greater oral bioavailability than 17-AAG [7]. The biological activity of the derivate has recently been demonstrated in xenograft tumor models [8, 9]. Data from preclinical toxicity studies for 17-DMAG in animal models have recently become available [10] and phase I clinical trials are being performed [11]. Most recently, fully synthetic, small molecule inhibitors of Hsp90 have been developed [12].

Despite a decreasing incidence due to widespread screening programs in most developed countries, carcinoma of the uterine cervix remains a major cause of cancer mortality ranking as the second most common cancer among women worldwide with an estimated 493,000 new cases and 274,000 deaths in the year 2002 [13]. Cervical cancer occurs at all ages including a relatively young age group, and sexual transmission of human papilloma virus (HPV) is the major aetiological factor [14]. A recent study underlined the increased long-term risk for invasive cervical cancer in woman after treatment of cervical intraepithelial neoplasia [15], and even after radical hysterectomy for FIGO IB1 recurrent disease will develop in about 20% of patients [16].

In this study we investigated the response of a panel of cervical carcinoma cell lines in vitro and in vivo to determine potential factors that might influence the sensitivity towards Hsp90 inhibition. A comparison with immortalized and normal human keratinocytes was performed since it had been suggested that the cell cycle changes induced by Hsp90 inhibitors are dependent on a functional Retinoblastoma

(Rb) pathway, a view that has recently become contested [17]. Also, the heat shock factor-1-dependent up-regulation of cytoprotective chaperones including Hsp70 and Hsp27 has been implicated with resistance mechanisms towards Hsp90 inhibitors [18–20]. It remains unclear, however, to what extent this particular mechanism and/or other factors contribute to the response observed with Hsp90 inhibitors in vivo. Hence, a better understanding of the complex changes induced by those compounds will help to identify factor(s) associated with clinical response or non-response and potentially explain the varying biological activities observed with different in vivo models [9]. Our results indicate that despite excellent sensitivity of the carcinoma panel in vitro, the efficacy of Hsp90 inhibition with 17-DMAG in vivo is influenced by factors that may include a target modulation, a narrow therapeutic range by oral application and response-modifying effects conferred by the tumor environment in addition to the known induction of a heat shock response.

Materials and methods

Drugs and chemicals

Geldanamycin (Biomol, Plymouth Meeting, PA, USA) was dissolved in dimethyl sulfoxide (DMSO) to a concentration of 10 mM and aliquots were stored at -20°C until use. 17-(dimethylaminoethylamino)-17-demethoxygeldanamycin (17-DMAG, NSC707545) was supplied by the Cancer Therapy Evaluation Program of the National Cancer Institute (Rockville, MD, USA), stored at -20°C and freshly dissolved in water daily immediately before use. All other chemicals used were commercially available and of analytical grade.

Cell culture

SiHa, ME180, HeLa, CaSki cervical carcinoma and Ect1/E6E7 immortalized cells from the normal ectocervix were obtained from American Type Culture Collection (ATCC, Manassas, VA, USA) and cultured in the recommended media to a maximum of 15 passages. Normal human epidermal keratinocytes (NHK) were purchased from Cambrex Bio Science (Walkersville, MD, USA) and cultured in Clonetics® keratinocyte growth medium supplemented with bovine pituitary extract according to the instructions provided by the supplier. Low passage NHK cells (≤ 4 passages) were used for all experiments. Cell cultures were regularly checked by staining with Hoechst33342 (Sigma-Aldrich, Oakville, ON, Canada) and microscopy to confirm absence of *Mycoplasma* contamination. Cell counts were performed using a Z1™ Coulter Counter® (Beckman Coulter,

Inc., Mississauga, ON, Canada). Doubling times (t_{Δ}) were estimated based on three independent experiments with each cell line. Four cell counts were obtained from exponentially grown cultures at 24 h intervals and the following equations were applied: (1) $N = N_0 e^{kt}$ and (2) $t_{\Delta} = \ln 2/k$. Cell culture under hypoxic conditions was performed as previously described [21]. Briefly, 96 well culture plates were exposed to a 0.2% oxygen atmosphere or normoxia with 5% carbon dioxide in Modular Hypoxia Chambers (Billups-Rothenberg, Del Mar, CA, USA) for 48 h with a continuous gas flow of ~ 15 l/h.

Live-cell imaging

A high-contrast live-cell imaging system (LCIS) manufactured by Richardson Technologies, Inc. (Toronto, ON, Canada) was used as previously described [22]. Briefly, a suspension of $\sim 5 \times 10^6$ SiHa cells in 1 ml culture medium was loaded into a collagen-coated chamber slide and placed onto the pre-warmed microscope stage. The sample space temperature was maintained at 37°C. Medium perfusion was started after cell adherence with conditioned medium obtained from exponentially grown SiHa cultures. Geldanamycin was added to the medium at a final concentration of 100 nM after an initial 24 h observation period, and changes in cell behavior and morphology were observed for up to 72 h. Images were captured at a rate of 1 frame per 3 min, and QuickTime movie files were generated from each image series. Image series were generated using Final Cut Pro software (Apple Computer, Inc., Cupertino, CA, USA).

Cell proliferation assays

Between 2×10^3 and 6×10^3 cells per well were seeded into 96-well cell culture plates based on initial experiments performed to determine the appropriate density for each cell line and assay. Geldanamycin, 17-DMAG or carrier were added to each well 24 h after cell culture was started. Cells were cultured for 48 h in presence of drug. Cell Titer 96® AQueous One [3-(4,5-dimethylthiazol-2-yl)-5-(3carboxymethoxyphenyl)-2-(sulfophenyl)-2H-tetrazolium, inner salt; MTS] (Promega, Madison, WI, USA) was used according to the instructions of the manufacturer. As a second assay, independent of the bioreductive capacity of the cells, crystal violet staining with a 0.5% [w/v] solution (Sigma–Aldrich) in 20% [v/v] methanol was used in parallel. A separate 96 well plate was stained with each crystal violet assay to determine pre-treatment values at the start of drug treatment. Elution of the crystal violet dye was performed with a 1:1 solution of 0.1 M sodium citrate and ethanol. Absorbance was measured at a wavelength of 490 nm for MTS and 570 nm for crystal violet using a Multiskan

EX spectrophotometer (Thermo Electron Corporation, Waltham, MA, USA).

Electrophoresis and immunoblotting

Whole cell lysates were prepared from subconfluent cultures treated with 1 μ M geldanamycin or 17-DMAG. Monolayer cell cultures and tumor xenografts were lysed with 50 mM Hepes-buffer, pH 8.0, containing 10% [v/v] Glycerol, 1% [v/v] Triton-X 100, 0.1% [v/v] sodium dodecylsulfate, 150 mM NaCl, 1 mM EDTA, 1.5 mM MgCl₂, 100 mM NaF, 20 mM NaP₂O₇, two tablets “complete” protease inhibitor cocktail (Roche, Penzberg, Germany) per 10 ml buffer. Samples were incubated with 4x sample buffer (200 mM Tris-buffer, pH 6.8, with 8% [w/v] sodium dodecylsulfate, 40% glycerol, 15% [v/v] 2-mercaptoethanol and 0.1% [w/v] bromophenol blue) at $\sim 95^{\circ}\text{C}$ for 5 min. Separation by sodium dodecylsulfate polyacrylamide gel electrophoresis and Western blot detection were performed as previously described [21]. Nitrocellulose membranes were probed with antibodies directed against Akt, Akt [pS473], Akt [pT308], Cdc2, Cdc2 [pY15], Myt1, Wee1, Plk1 (208G4), Cyclin B1 (V152), PARP, Rb (4H1) (Cell Signaling Technology, Danvers, MA), Histone H3 [pS10] (Upstate/Millipore, Billerica, MA, USA), GAPDH (6C5) (Ambion, Austin, TX, USA), p-glycoprotein (MDR Ab-2, F4) (Lab Vision, Fremont, CA, USA), Hsp90 α (9D2), Hsp90 (16F1), Hsp27 (G3.1) (Nventa, Ann Arbor, MI, USA) and p53 (Bp53-12) (Santa Cruz Biotechnology, Santa Cruz, CA, USA). Signal detection after incubation with secondary antibodies (GE Healthcare-Amersham, Buckinghamshire, UK or Nventa) was performed with SuperSignal® West Pico chemiluminescent substrate (Pierce, Rockford, IL, USA). Quantification of Western blot signals was performed using the Typhoon™ 9410 imaging system (GE Healthcare, Buckinghamshire, UK) with ECL plus Western blotting reagents and Image Quant 5.2 software. Image Quant analysis was performed by calculating an index based on signal intensity multiplied by signal area.

Flow cytometry

Cell death due to Hsp90 inhibition was measured using a Hoechst33342/propidium iodide flow cytometric assay. 5×10^4 to 1×10^5 cells were seeded into 6-well culture plates (Nunc, Roskilde, Denmark) and grown for 24 h before treatment with geldanamycin (10–5,000 nM) or DMSO ($\leq 0.1\%$) as control for 48 h. Floating and adherent cells were collected and stained with 10 $\mu\text{g}/\text{ml}$ Hoechst33342 (20 min, 37°C). Five $\mu\text{g}/\text{ml}$ propidium iodide (Sigma–Aldrich) was added 5 min before analysis. For cell cycle analysis the cells were harvested, resuspended

in medium, permeabilized with 0.1% Triton X-100 and stained with 1 µg/ml 4',6-diamidino-2-phenylindole (DAPI) for 30 min. Human lymphocytes were used as DNA standard. DNA histograms were analyzed using ModFit LTTM (Verity, Topsham, ME). To test for a potential multi-drug resistance phenotype, a functional and an immunofluorescence-based assay were performed with all cell lines essentially as described [23]. For the latter assay phycoerythrin-conjugated anti-CD243 (Beckman-Coulter, Mississauga, ON, Canada) was used. CCRF-CEM T-lymphoblastic cell line and the vinblastine-resistant variant VLB 1.0 were used as negative and positive controls for flow cytometry and Western blot confirmation, respectively. Analysis was performed using either a LSR II (BD Biosciences, San Jose, CA, USA) or an Epics Elite flow cytometer (Beckman-Coulter, Miami, FL, USA).

Animal xenografts

Female severe combined immunodeficient (SCID) mice were obtained from an in-house breeding program. Animals were housed at the Ontario Cancer Institute animal facility and had access to food and water *ad libitum*. All experiments were done under protocols approved according to the regulations of the Canadian Council on Animal Care. (Animal weight loss and tumor mass not exceeding 20 and 10% of normal bodyweight, respectively.) Tumor xenografts were initially grown from suspensions of ME180 and CaSki cells (ca. 1.5×10^6) injected into the left hindleg. As the tumors approached 10 mm in diameter the donor mice were killed and tumor fragments of ~ 3 mm diameter were implanted into the flanks of recipient mice. This procedure ensured a similar size of all xenografts during the treatment. Tumor growth was monitored with caliper measurements and tumor volumes were determined according to the formula: $\text{Width}^2 \times \text{Length}/2$. Treatment was started at a mean tumor volume of $\sim 200 \text{ mm}^3$ in the recipient mice. 17-DMAG was given at 6 or 10 mg/kg dose twice daily by oral gavage in cycles of 5 consecutive days with 2 days interval between each cycle. Control mice received water on the same schedule. All mice were killed on day 30 (ME180) or day 22 (CaSki) after commencement of the study by cervical dislocation ~ 4 h after the last treatment, and immediately sampled for plasma and tumor tissue. Tumors were explanted and dissected to obtain 4 samples (snap frozen in liquid nitrogen, tumor cell lysate, formalin-fixed for paraffin-embedding, embedded in optimum cutting temperature medium) from each xenograft. Percent tumor growth inhibition at the end of the study was calculated based on the mean tumor volumes of each group with following equation: $(1 - [\text{treated}/\text{control}]) \times 100$.

Immunohistochemistry

Tumor tissue was fixed overnight in 10% neutral buffered formalin, embedded in paraffin and cut into 4 µm sections that were processed by standard procedures. The following primary antibodies and dilutions were used: Hsp27 (1:2,000) (G3.1) (Nventa), Akt [pS473] (736E11) (1:100), Akt [pT308] (244F9) (1:100) (Cell Signaling Technology), HIF-1 α (clone54) (1:400) (BD Transduction Laboratories, San Diego, CA, USA). Immunohistochemistry was carried out after primary antibody incubation with linking and labeling reagents (IDetect Ultra HRP Detection System, ID Labs, London, ON, Canada) for 30 min each followed by diaminobenzidine (Dako, Carpinteria, CA, USA) for 5 min. Sections were counterstained with Gill modified hematoxylin and coverslipped with Permount* Mounting Medium (Fisher Scientific, Nepean, ON, Canada).

High performance liquid chromatography (HPLC)

17-DMAG was measured in tumor tissues using a HPLC method as previously described [7]. Briefly, tumor samples were homogenized in 2.5 ml phosphate-buffered saline (PBS) and extraction was performed with 2.5 ml of a 1:1 solution of ethyl acetate and methyl-tert-butyl ether added to 1.25 ml homogenate. Samples were then centrifuged at 3,000 rpm for 10 min. Supernatants were separated and dried using a Universal Vacuum system (Thermo Electron Corporation). Residues were reconstituted with 0.3 ml of a 2:1 solution of methanol and water. Fifty microliter of the final sample was injected into a LC-10AD liquid chromatography system equipped with a SPD-10A UV detector (Shimadzu Scientific Instruments, Kyoto, Japan). Separation of 17-DMAG and internal standard was achieved at ambient temperature using a Symmetry[®] C18 reverse-phase analytical column (150 × 4.6mm, 5 µm particles) protected by a Symmetry[®] C18 guard column (Waters Associates, Milford, MA, USA). The isocratic mobile phase consisted of acetonitrile:25 mM potassium phosphate (30:70, v/v), pH 5.0, with 0.2% triethylamine and was pumped at a flow rate of 1.0 ml/min. The detector was set to a wavelength of 330 nm. Data were collected and analyzed using Shimadzu Class VP software (VP 7.1.1 SP1). Run time was 30 min. The retention times of 17-DMAG and OSI-420 (internal standard) were approximately 6.6 and 14.7 min, respectively. Calibration curves were prepared with 10–1,000 ng/ml 17-DMAG.

Statistical analysis

All experiments were performed at least three times. Statistical analysis of in vitro data was performed using Student's *t* test. Data obtained from the xenograft model

(tumor volume and animal weight) were analyzed using mixed modeling. To stabilize the variance of the residuals the tumor volume was transformed and the model was performed on the cubic root of the volume. *P* values of < 0.05 were considered statistically significant.

Results

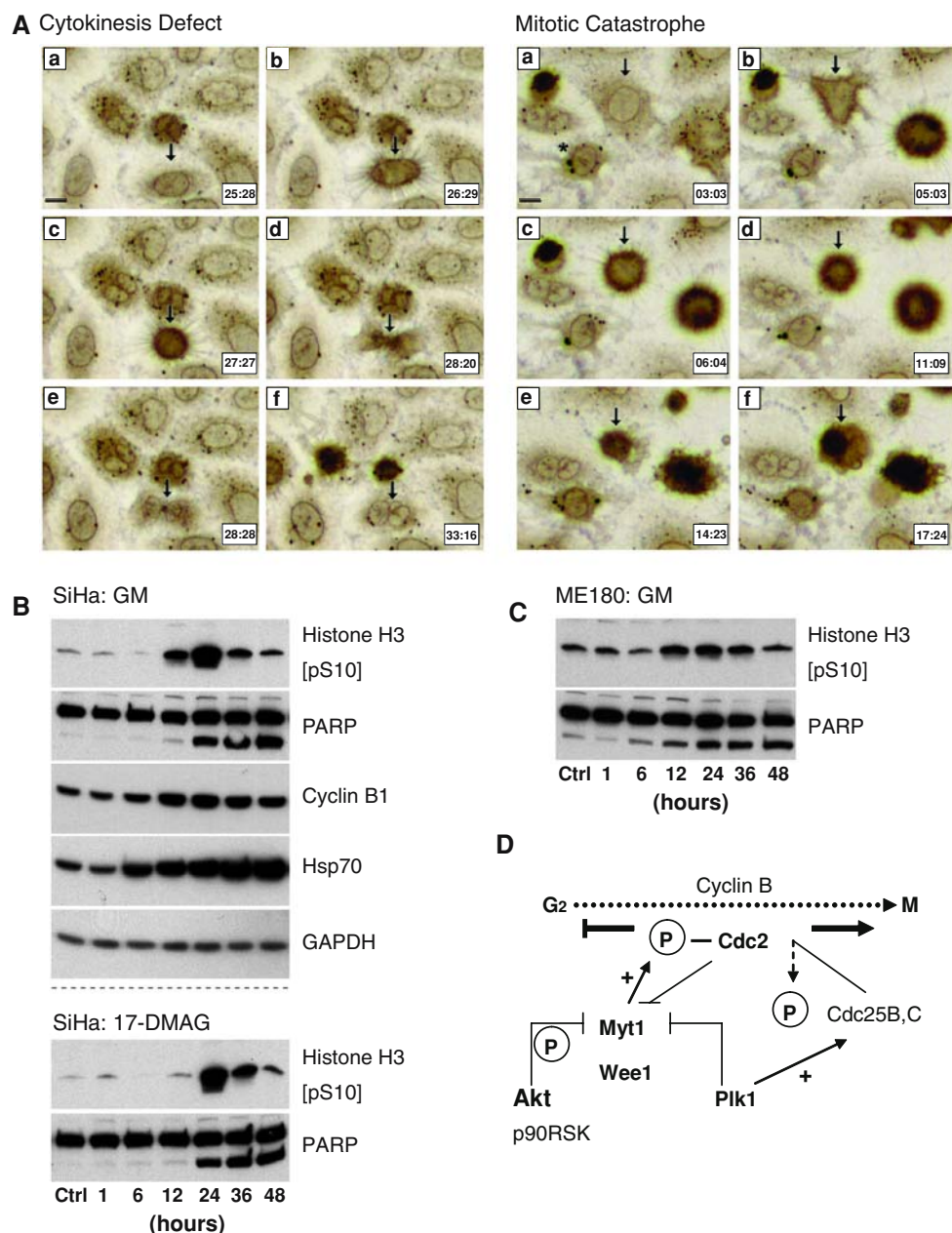
Abnormal cytokinesis and mitotic catastrophe occur due to Hsp90 inhibition

To examine the changes in cell behavior and morphology induced by Hsp90 inhibitor treatment, SiHa cells were

Fig. 1 Hsp90 inhibition causes a cytokinesis defect and apoptosis by mitotic catastrophe. **A** The cytokinesis defect (A: left panel, images a–f, arrow) gives rise to bi-nucleated cells. Mitotic catastrophe (A: right panel, images a–f, arrow) occurs after prolonged M-phase (~9 h), and complex changes in cell morphology can be observed in other cells (A: right panel, image a, asterisk). Time is indicated as hours:minutes after treatment start in the right lower corner of each image. Size bars equal 10 μ m. **B** Treatment of SiHa cells with 1 μ M geldanamycin or 17-DMAG causes a sequential increase of phosphorylated Histone H3, Cyclin B1 and cleaved PARP. The increase of Hsp70 indicates the heat shock response induced by the treatment. *Ctrl* control; duration of treatment as indicated in hours. **C** Treatment of ME180 cells with 1 μ M geldanamycin causes an increase of phosphorylated Histone H3 and cleaved PARP similar to SiHa cells. **D** Schematic of the G2/M transition. Factors that are recognized Hsp90 clients are highlighted (*bold print*) and include a number of kinases that control the transition of cells from G2 to M phase

cultured in a live-cell imaging system. Addition of 100 nM geldanamycin to the perfusion medium resulted in abnormalities of cytokinesis with dumbbell-shaped nuclei and occurrence of bi-nucleated cells (Fig. 1A: Cytokinesis Defect). Cells undergoing mitosis remained in a rounded state for a prolonged period (Fig. 1A: Mitotic Catastrophe) before undergoing cell death, which was indicative of mitotic catastrophe. In addition, complex alterations of the cell morphology were observed with increasing duration of drug exposure (Fig. 1A, asterisk) which was most likely due to the degradation of client factors such as FAK and Src that control cell shape and motility.

Biochemical evidence for the mechanism of cell death was obtained from a time-course experiment during which



SiHa and ME180 cells were exposed to 1 μ M geldanamycin or 17-DMAG for time periods up to 48 h (Fig. 1B + C). Both cell lines responded with a sequential increase of phosphorylated Histone H3 and occurrence of cleaved poly (ADP-ribose) polymerase (PARP) 12–24 h after start of the treatment. SiHa cells also showed a transient increase of Cyclin B1. Hsp70 levels increased as consequence of the heat shock response induced by the treatment.

Entry of eukaryotic cells into M phase is regulated by activation of Cdc2 kinase (Fig. 1D). Phosphorylation and inhibition of Cdc2 is carried out by Myt1 and Wee1, dephosphorylation and activation by Cdc25 phosphatase. Multiple kinases regulating this transition are recognized Hsp90 client factors, which provides a possible rationale for the observed mechanism of cell death [24].

Cell death due to Hsp90 inhibition is modified by factors other than proliferation rate

If cell death due to Hsp90 inhibition was solely dependent on the proportion of cells entering mitosis, then the drug response should be directly correlated with surrogates of the proliferation rate (e.g., doubling time). To test this hypothesis a panel of cervical carcinoma cell lines was treated with increasing concentrations of geldanamycin and the proportion of non-viable cells was measured 48 h after treatment start based on an increased plasma membrane permeability for propidium iodide. HeLa and SiHa cells displayed cell death with a proportion of \sim 15% non-viable cells after 48 h, whereas a proportion of \sim 30% was measured for CaSki and ME180 (Fig. 2a). The observed response remained relatively constant across the concentration range of 100–5,000 nM lending further support to the hypothesis that cell death within 48 h after treatment start occurred in a proliferation-dependent fashion. An estimate of the individual doubling times of the cell lines revealed, however, that the proliferation rate was unlikely the sole factor determining the response towards Hsp90 inhibition. HeLa cells with an in vitro doubling time of 21 h responded more similar to SiHa cells, which had with 37 h the longest doubling time in the panel (Table 1). The observed differences between the cell lines were not due to multi-drug resistance drug transport proteins whose absence was confirmed by flow cytometry and Western blotting (data not shown). Thus, additional factors are likely to modify the response towards Hsp90 inhibition.

It has previously been shown that normal cells can be less sensitive to Hsp90 inhibition than malignant cells [2]. These experiments were performed with a comprehensive panel of different cell lines. However, normal and immortalized keratinocytes, the counterparts of malignant squamous carcinoma cells were not previously tested. Hence, we performed proliferation assays to estimate the IC_{50} values for the carcinoma

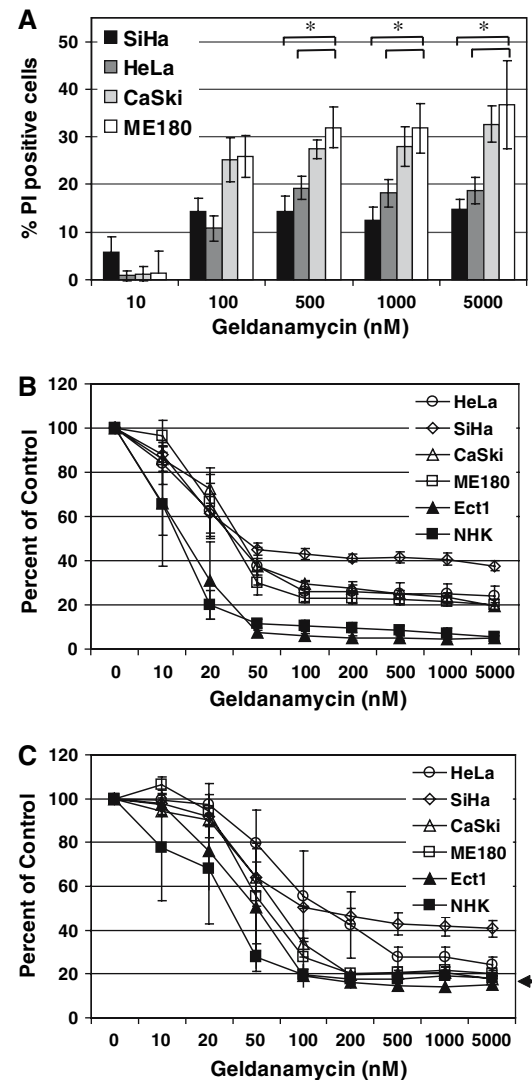


Fig. 2 Hsp90 inhibition causes cell death and growth inhibition in a cell line specific manner. **a** The proportion of non-viable cells after 48 h of treatment with geldanamycin was determined by flow cytometry based on Hoechst33342/propidium iodide staining. (* $P < 0.005$; bars, SEM) **b + c** The drug-response curves of geldanamycin-treated cervical carcinoma cells (HeLa, SiHa, CaSki, ME180), immortalized keratinocytes (Ect1/E6E7) and normal keratinocytes (NHK) were determined based on MTS (**b**) and crystal violet assay (**c**). Data points are mean values of 3 independent experiments performed with triplicates; bars, SEM. The arrow in **c** indicates the average value at the start of drug treatment

cell line panel as well as E6/E7-immortalized and normal keratinocytes. Two assays were performed in parallel, a tetrazolium-based (MTS) assay relying on the bio-reductive capacity of the cells and a purely colorimetric (crystal violet) assay which measured the amount of cell protein that remained attached in the 96-well plate after treatment. For the latter assay the pre-treatment value, i.e., the amount of cell mass at the time point of inhibitor addition to the culture, was measured. As expected, the IC_{50} values for the

Table 1 Doubling times of the cell line panel and IC_{50} values for Hsp90 inhibition with geldanamycin

Cell line	Doubling time Mean \pm SD (h)	IC_{50} (MTS) Mean \pm SD (nM)	IC_{50} (Crystal) Mean \pm SD (nM)
HeLa	21.3 \pm 1.6	35.2 \pm 12.3	139.8 \pm 115.6
SiHa	36.6 \pm 1.7	26.1 \pm 11.8	52.5 \pm 22.9
CaSki	30.3 \pm 1.8	37.3 \pm 6.8	74.7 \pm 25.5
ME180	26.9 \pm 1.6	32.5 \pm 13.5	63.0 \pm 41.9
Ect1/E6E7	26.7 \pm 1.6	22.9 \pm 13.8	56.1 \pm 39.4
NHK	N.D.	17.1 \pm 8.2	33.9 \pm 22.8

IC_{50} values were calculated based on two different assays indicated as MTS and Crystal

N.D. not determined

carcinoma panel fell within a range of 26–37 nM based on the tetrazolium assay and 53–140 nM based on the crystal violet assay (Table 1; Fig. 2 b + c). The difference between the two assays was expected since a low dose treatment may require a longer time period to cause growth inhibition despite compromised viability at the endpoint. However, the sensitivity of the immortalized and normal keratinocytes with IC_{50} values of 23 and 17 nM (MTS), respectively, was an unexpected result and not due to a higher proliferation rate of these cells. Furthermore, SiHa cells seemed to retain a limited ability to proliferate even in the presence of Hsp90 inhibitor as indicated by a higher plateau value in the concentration range of 0.2–5 μ M (Fig. 2b + c). This could be due to the longer doubling time of these cells, which may permit a limited repair or bypass of some inhibitor-induced effects.

Hsp90 inhibition affects multiple cell cycle regulators of the G2/M transition

To further explore the cell cycle-related effects that may be associated with a differential sensitivity towards Hsp90 inhibition, the cell cycle distribution in cervical carcinoma cells and keratinocytes after treatment with 1 μ M geldanamycin was examined. In all cells, irrespective of their pre-treatment level of Retinoblastoma protein, an increase of the G2/M fraction of the cell cycle was observed 24 h after treatment start (Figs. 3, 4 [Rb: arrow]). This increase was most pronounced in CaSki cells, whereas HeLa, SiHa, ME180 and Ect1/E6E7 cells showed very similar distributions. NHK cells displayed a relatively small increase of the G2/M fraction, and an inverse relationship of the G2/M response with increasing passage number was noticed (data not shown). The increase of the G2/M fraction was manifest in all cell lines at 24 h and only minimal changes were observed thereafter (48 and 72 h) suggesting a complex cell cycle-inhibitory effect of the treatment (data not shown).

Western blotting for regulators of the G2/M transition as well as Akt, a protein kinase with important pro-survival functions and dependency on Hsp90 chaperone activity, was performed to gain insight into differences between the cell lines that might provide an explanation for the varying rates of cell death. A rapid degradation of multiple cell cycle regulatory kinases as well as a decrease in Akt protein levels and phosphorylation was observed within 24 h of treatment (Fig. 4). Apart from a pronounced decrease of Cdc2, a destabilization of the negative G2/M regulators Myt1 and Wee1 was observed. A high molecular weight form of Myt1 corresponding to the hyperphosphorylated, inactive molecule was observed in SiHa, CaSki, ME180 and Ect1/E6E7 cells. An increase in phosphorylated Histone H3 [pS10] was observed in SiHa, CaSki and ME180 indicating that cells proceed into M phase during the first 24 h of inhibitor treatment (Fig. 4, arrowheads). Plk1 is a positive regulator of the G2/M transition and has been recognized previously as a Hsp90 client [25]. Surprisingly, Plk1 remained relatively stable within 24 h in most of the cell lines used in this study except NHK. Normal cells displayed a loss of all G2/M regulators within 24 h after treatment start and no increase in phosphorylated Histone H3 was observed. The occurrence of the cleaved form of PARP (Fig. 4, asterisk) indicated, however, that apoptosis as a consequence of Hsp90 inhibition was triggered in all cell lines.

Interestingly, ME180 and Caski cells, which showed a higher proportion of cell death, as well as Ect1/E6E7 and NHK had much higher pre-treatment levels of active Akt compared to SiHa and HeLa cells (Fig. 4, dotted line). Akt is a positive regulator of cell proliferation and survival involved in a complex signaling network and has also been recognized in its role as one of the kinases that mediate Myt1 hyperphosphorylation [26]. Thus, high levels of Akt activity might be a potential predictor for an efficient induction of cell death due to Hsp90 inhibition. The increase Hsp27 in all cell lines was consistent with an expected heat shock response and confirmed the effective inhibition of Hsp90.

Diminished efficacy of Hsp90 inhibition in vivo is associated with alterations in target abundance and activity

ME180 and CaSki cells were grown as subcutaneous tumor xenografts in SCID mice in order to test their response towards Hsp90 inhibition in an in vivo model. 17-DMAG has properties such as its oral bioavailability that make this substance particularly attractive, and in vivo growth-inhibitory effects of the derivate have recently been shown [9]. In vitro proliferation assays performed with ME180 to compare geldanamycin and 17-DMAG indicated an IC_{50} of 17-DMAG that was approximately twofold higher, but still below 100 nM by MTS assay (data not shown).

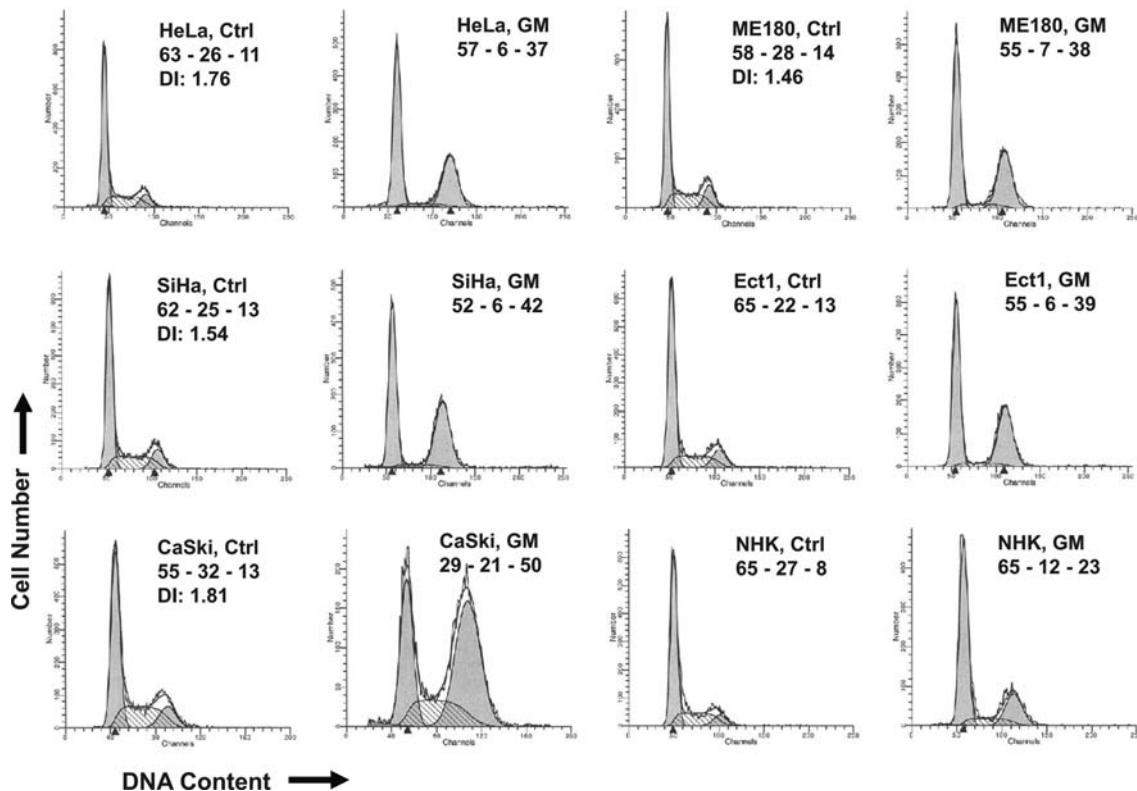


Fig. 3 Cell cycle response of geldanamycin-treated cervical carcinoma cells (HeLa, SiHa, CaSki, ME180), immortalized keratinocytes (Ect1/E6E7) and normal keratinocytes (NHK). Percent cells in G1-S

G2/M phase are given for control (*Ctrl*) and treatment (GM: 1 μ M geldanamycin, 24 h). *DI* DNA index

17-DMAG was given by oral gavage at two different dose levels, 6 and 10 mg/kg, twice daily for 5 days per week to treat the ME180 xenografts. The higher dose level was close to the maximum tolerated dose for chronic application as previously reported [9], and a statistically significant weight loss was detected in this group (ME180: $P < 0.0001$). Gastrointestinal complications were observed in separate experiments in mice for which this dose was surpassed. Despite confirmed in vitro sensitivity, no statistically significant tumor growth inhibition was detected with ME180 (10 mg/kg 17-DMAG: $P = 0.10$, 6 mg/kg 17-DMAG: $P = 0.92$, $n = 9$ animals/group; Fig. 5a). These results were confirmed using CaSki xenografts treated with 10 mg/kg 17-DMAG twice daily (weight loss: $P = 0.023$, growth inhibition: $P = 0.43$, $n = 6$ animals/group; data not shown). Comparison of treatment (10 mg/kg) and control groups at the end of the study showed a very limited effect with a reduction in tumor volume of 21 and 18% for ME180 and CaSki, respectively.

To confirm drug delivery into the tumor, HPLC analysis for 17-DMAG was performed on snap-frozen tissue samples from the ME180 xenografts acquired approximately 4 h after the last drug application. A mean concentration of 490 ng/g (standard deviation: 102 ng/g) and

595 ng/g (standard deviation: 142 ng/g) was measured for the low and the high dose treatment group, respectively. This corresponds to approximately 794 and 964 nM 17-DMAG (molecular weight: 617). Thus, Hsp90 inhibition with 17-DMAG showed a relative lack in efficacy in vivo as compared to in vitro in this model.

Western blotting performed with tumor lysates to detect Akt protein and phosphorylated Akt [pT308] showed a trend towards lower levels in the treated group of the ME180 xenografts. Hsp27 and Hsp70 were slightly increased consistent with a heat shock response induced by Hsp90 inhibition (Fig. 5b + c). However, conspicuously lower levels of Hsp90 as well as lower phosphorylated Akt [pT308] were detected in all ME180 xenograft tumors compared to monolayer cell cultures (Fig. 5b, arrows). Lower levels of Hsp90 were also detected in CaSki xenografts compared to cultured cells. This result was confirmed with a second antibody which detects both isoforms of Hsp90, α and β , albeit with a somewhat weaker signal. In addition, lower levels of Cyclin B1 were detected in tumors compared to cell culture indicative of changes in cell proliferation that might have an impact on the response towards Hsp90 inhibition.

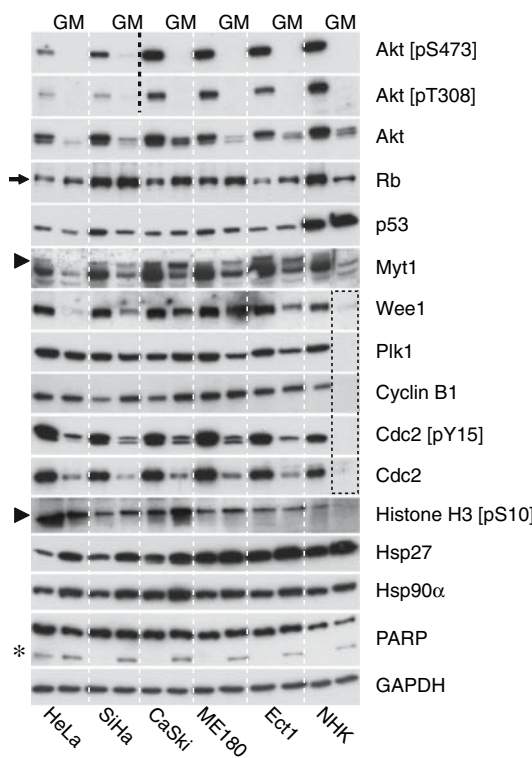


Fig. 4 Hsp90 inhibition leads to a rapid decrease of Akt protein levels and activity as well as cell line specific alterations of the G2/M transition. Western blot analysis for Akt and G2/M regulatory factors in geldanamycin-treated cervical carcinoma cells, immortalized and normal keratinocytes. Treatment with 1 μ M geldanamycin for 24 h is indicated at the top of the panel (GM). Pre- and post-treatment levels of Akt are shown. HeLa and SiHa cells display lower levels of pre-treatment Akt activity compared to the other cell lines of the panel (dotted line). A range of cell line specific levels of Retinoblastoma (Rb) protein was detectable (arrow). Hyperphosphorylated Myt1 and an increase in phosphorylated Histone H3 indicate entry into mitosis (arrowheads). Cleaved PARP indicates apoptotic cell death (asterisk). The loss of multiple G2/M regulators in NHK cells due to Hsp90 inhibition is highlighted (dotted box)

The tumor environment potentially contributes to an altered efficacy of Hsp90 inhibition with 17-DMAG

Immunohistochemistry performed for phosphorylated Akt on ME180 xenograft sections revealed an accentuated staining in tumor cells adjacent to the blood vessel containing stroma islets. A decrease in staining intensity for phosphorylated Akt [pS473] was most noticeable in those perivascular areas if treated tumors were compared to control (Fig. 6a + b, highlighted areas). However, high levels of Akt phosphorylation were maintained at the invasion front (Figure 6b, insert). No obvious changes in staining pattern could be discerned for Hsp27. Thus, changes in abundance of primary and/or secondary target(s) as well as a potential lack of response at the periphery of the xenografts may contribute to a relative drug resistance in vivo.

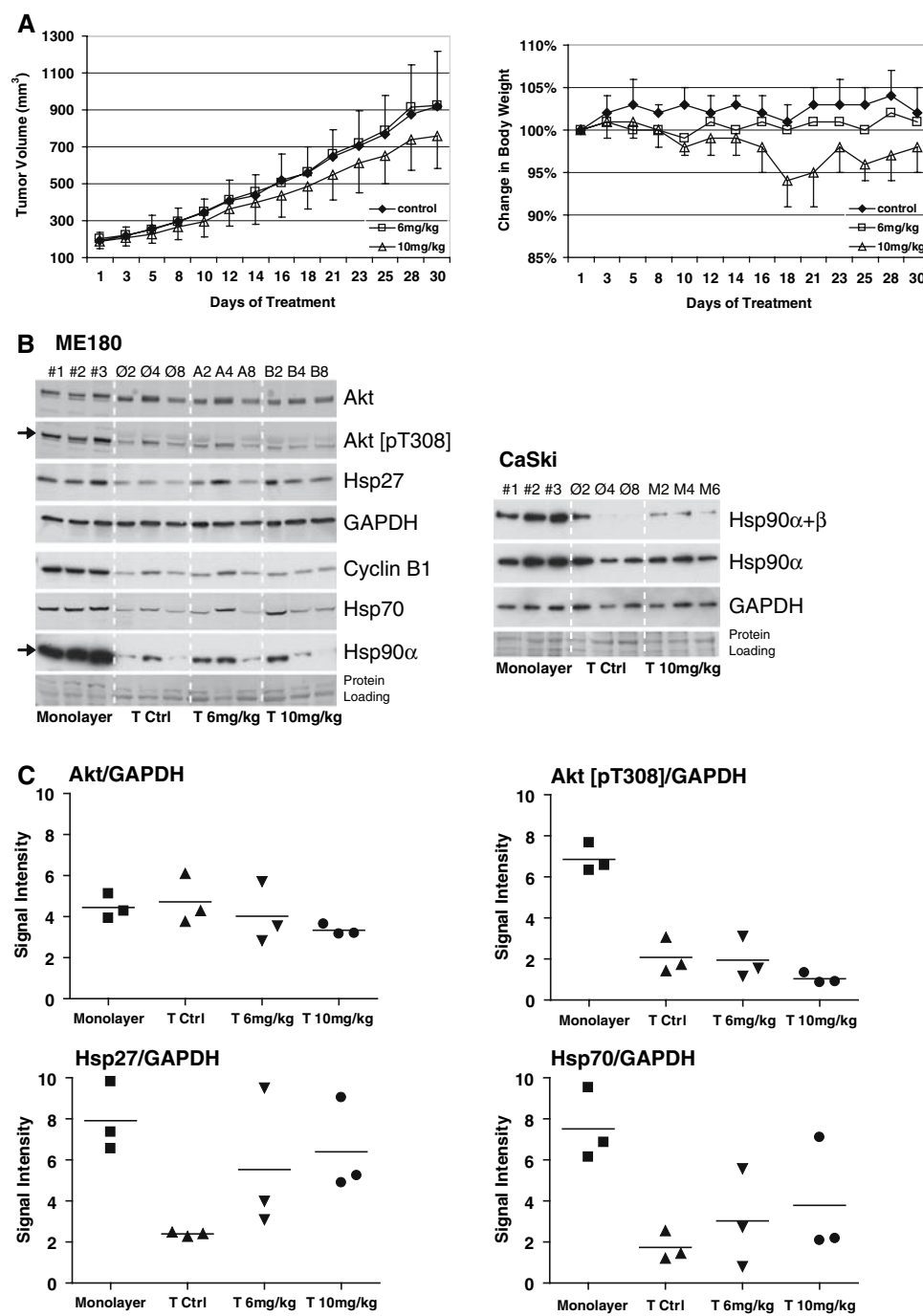
Recently it has been reported that low doses of Hsp90 inhibitors can cause an induction of the hypoxia-inducible factor system with increased activity of the heterodimeric transcription factor HIF-1 [27]. In agreement with those results we had previously observed that low doses of geldanamycin can induce an increase of the Hsp90 dependent regulatory subunit HIF-1 α [21]. Interestingly, the xenograft tumors examined in this study showed extensive necrotic areas in all groups, presumably due to hypoxia and nutrient deprivation. Consistent with that, a marked induction of HIF-1 α was observed in all ME180 xenografts independently of the treatment (Fig. 6c). To test if exposure to low doses of Hsp90 inhibitors may be able to protect cells from the adverse effects of hypoxia, we performed proliferation assays for geldanamycin and 17-DMAG with cells cultured for 48 h under 0.2% oxygen. Exposure of ME180 cells to the Hsp90 inhibitors geldanamycin (data not shown) and 17-DMAG (Fig. 6d) at very low concentrations (5–10 nM) caused a slight pro-proliferative effect compared to control under hypoxic conditions. Although clearly higher doses of 17-DMAG were measured in our xenografts by HPLC, this result suggests that Hsp90 inhibition in the context of a hypoxic environment may result in unpredicted changes in net sensitivity if tumor areas are not exposed to sufficient concentrations of the inhibitor during the entire course of the treatment.

Discussion

We show here that Hsp90 inhibition effectively induces apoptosis and growth arrest in a panel of cervical carcinoma cell lines in vitro. However, application of the orally bioavailable Hsp90 inhibitor 17-DMAG had only limited growth inhibitory effects in two in vitro-sensitive cell lines tested as subcutaneous xenografts. This may be due to (1) differences in abundance of the primary (Hsp90) and the activity of secondary (e.g., Akt) targets, (2) a narrow therapeutic range by oral application preventing further dose-escalation, (3) response-modifying factors within the tumor environment (e.g., drug penetration, tissue hypoxia) or (4) a combination of the factors mentioned above.

Hsp90 is involved in a broad array of vital cellular processes by maintaining the functional conformation of different signal transduction factors involved in growth control, survival and development. Increasing insight into the biology of this unique chaperone suggests that Hsp90 could be a more effective target in oncology than single-pathway oriented strategies whose success might be hampered by the evolution of new cell clones and the plasticity inherent to signal transduction networks in tumor cells. In addition, studies performed with different biological model systems provide compelling data that suggest a role

Fig. 5 Efficacy of Hsp90 inhibition in a subcutaneous model treated with 17-DMAG by oral application. **a** Change in ME180 xenograft tumor volume and animal body weight ($n = 9$ animals/group). Data points represent mean values; bars, SD. **b** Western blots were performed with lysates of monolayer cell cultures and xenograft samples obtained for ME180 and CaSki. Note the lower levels of Hsp90 α and phosphorylated Akt [pT308] (arrows) despite comparable levels of Akt protein, GAPDH and equal protein loading confirmed by amido black staining of the blot membranes. **c** Western blot signals were quantified and the values were normalized with GAPDH as loading control. Symbols indicate individual data points; horizontal bars the mean for each group. *T Ctrl*: control xenografts; *T 6 mg/kg*, *T 10 mg/kg*: xenografts treated with different dose levels of 17-DMAG. Signal intensity: arbitrary units



of the chaperone during evolutionary processes, which may also occur during tumor progression [17]. Thus, the targeting of Hsp90 has become a focus of current drug-development efforts.

Despite the success of screening programs in developed countries, carcinoma of the uterine cervix still represents a global health problem, and therapeutic options for patients with distant spread or recurrent disease are limited [28]. Few studies have focused so far on chaperone proteins in cervical carcinoma [29] and, to the best of our knowledge, no study has systematically explored the effects of Hsp90

inhibitors in cervical carcinoma cells and their benign counterparts. Our results show that cervical carcinoma cells display a nanomolar range of sensitivity towards Hsp90 inhibition with growth inhibition and induction of apoptotic cell death. At least part of the apoptotic response can be attributed to a dysregulation of kinases responsible for the coordinated execution of mitosis. Similar results have previously been obtained for glioma cells [30] and interesting data recently published by Basto et al. [31] implicate Hsp90 in the targeting of Cyclin B to centrosomes and spindle microtubules during mitosis.

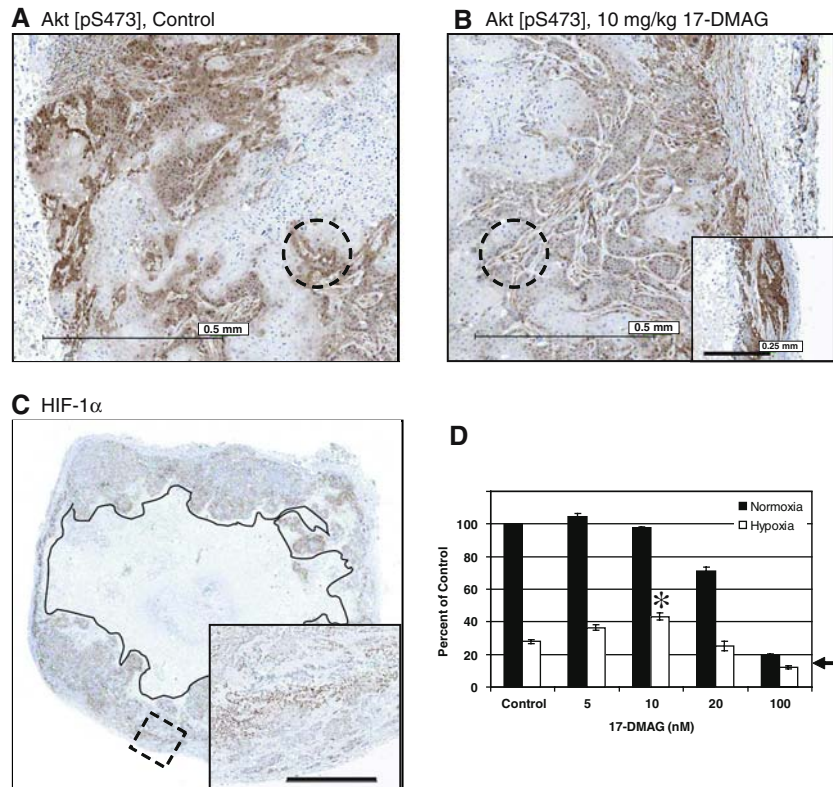


Fig. 6 Potential factors that may alter the in vivo efficacy of Hsp90 inhibitors include lack of client protein destabilization at the invasion front and tumor hypoxia. **a + b:** Phosphorylated Akt [pS473] detected by immunohistochemistry in two representative ME180 xenograft specimens of control and treatment group. Differences in staining intensity and pattern are noticeable in perivascular regions (dotted circles). Strong staining persists at the tumor periphery despite treatment (right panel, insert). Size bar in the insert equals 250 μ m. **c:** A large central necrotic core (outline) within a representative ME180 xeno-

graft and immunohistochemistry showing an accumulation of hypoxia-inducible factor-1 α (HIF-1 α) throughout the viable tumor area indicate the presence of tissue hypoxia. The dotted box corresponds to the magnified insert. Size bar in the insert equals 500 μ m. **d** Low dose treatment with the Hsp90 inhibitor 17-DMAG causes a slight pro-proliferative effect under hypoxic conditions. Data points are mean values of 6 experiments (crystal violet assay) performed with triplicates; bars, SEM. The arrow indicates the average value at the start of drug treatment. (* $P < 0.05$ compared to control under hypoxia)

The comparison performed with our cell line panel underlines, however, that factors other than mitotic catastrophe contribute to a differential cell line-specific response. Interestingly, a higher Akt activity was detectable in those cell lines that had a higher proportion of non-viable cells after treatment. Akt, also referred to as PKB (protein kinase B), plays a critical role in controlling the balance between cell survival and apoptosis [32], and inhibition of Hsp90 leads to a rapid dephosphorylation of the kinase [33]. Akt is also involved in cell cycle regulation via different pathways including the phosphorylation and inactivation of Myt1. This, however, does not exclude the contribution of other signal transduction pathways such as the MAPK pathway and its downstream factor p90RSK. Furthermore, it has been shown that the magnitude of cellular signals involving the Akt and the MAPK pathways can increase early during treatment with Hsp90 inhibitors [34], and we cannot exclude that this effect may contribute to the accumulation of cells in G2/M. This scenario is likely subject to drastic changes over time depending on the degradation kinetics of

individual client proteins, and the complex alterations associated with Hsp90 inhibition might prove difficult to unravel without the use of more comprehensive analytical techniques such as (phospho-) proteomic approaches. The apparent association between Akt activity and drug sensitivity, however, emphasizes the significance of the kinase as an important Hsp90 client despite the fact that the cell lines examined here were non-isogenic.

The sensitivity observed with normal and immortalized keratinocytes was somewhat unexpected since previous research pointed towards a greater resistance of non-malignant cell types [2]. However, these findings might have been influenced by the specific cell types chosen, as well as the type-specific life cycle of normal cells. Sanderson et al. recently reported that cell death due to Hsp90 inhibition in human vascular endothelial cells is dependent on the proliferative state, which is more in line with our results [35]. In addition, the drug-induced increase of the G2/M fraction observed with normal keratinocytes contradicts a previous model that associated the position of the cell cycle arrest

with the existence of alterations in the Retinoblastoma pathway. That this Rb-dependency might in fact be tumor/cell-type specific has also been pointed out in a recent review by Whitesell and Lindquist [17].

Despite confirmed sensitivity of the two selected cell lines in vitro, only a limited growth inhibitory effect was observed in the corresponding xenograft models treated close to the maximum tolerated dose level. The subsequent comparison between samples from monolayer cultures and xenografts revealed lower levels of Hsp90 in the latter which may be associated with a change in Hsp90 dependency for cell survival. In addition, a lower activity of Akt kinase was observed in xenografts indicating a combined modulation of primary and secondary target(s). A second potential contributor to the lack of in vivo efficacy is the tumor environment, which may influence drug distribution. The xenograft model used in our study tested the growth inhibitory effect of 17-DMAG on established tumors, which may be different from models that use an earlier administration of drug after subcutaneous inoculation of cell suspensions. Extracellular matrix structure and angiogenesis may play a role in this context.

The pro-proliferative effect observed in our study in monolayer culture was confined to an extremely low concentration range. However, possible pleiotropic effects of Hsp90 inhibitors under hypoxic conditions may need to be examined in further detail. Our results also strongly emphasize the need for more relevant in vitro models (e.g., 3-dimensional tissue culture, hypoxia and nutrient-deprivation models) for pharmacodynamic testing. Interestingly, experiments performed with orthotopic xenografts grown in the uterine cervix of mice indicated significantly higher tissue concentrations of 17-DMAG and more pronounced effects on client protein phosphorylation (J. Schwock, unpublished results).

Although the results described here may be interpreted as a caveat for the extrapolation of in vitro data towards in vivo models or even a clinical situation, cell lines will still remain the primary model to evaluate new therapeutics and to guide any research performed with more complex systems. For Hsp90 inhibitors of the benzoquinone ansamycin group a further careful examination of their potentially beneficial properties seems warranted to define their value for the treatment of different oncologic entities particularly in combination with other therapeutic modalities such as radiation [36, 37]. In addition, the development of novel Hsp90 inhibitors with a better therapeutic window [38, 39] as well as the largely unexplored effects of these compounds on tumor progression and metastasis development hold a significant potential and deserve in-depth examination in the future.

Acknowledgments 17-DMAG (NSC 707545) from Kosan Biosciences was supplied by the Cancer Therapy Evaluation Program of the National Cancer Institute (Rockville, MD). We are indebted to the research team of Richardson Technologies, Inc., particularly Bruno Chue, for their support with the live-cell imaging studies and data processing. We also thank Wen-Jiang Zhang and Dr. Xueyu Chen (Ontario Cancer Institute) for the HPLC measurements performed for 17-DMAG in xenograft samples and Melania Pintilie for help with the statistical analysis of the animal data. This study was supported by the Terry Fox Program Project Grant of the National Cancer Institute of Canada. J.S. was supported by the CIHR Training Program on Clinician Scientists in Molecular Oncologic Pathology (STP-53912).

References

1. Pratt WB, Toft DO (2003) Regulation of signaling protein function and trafficking by the hsp90/hsp70-based chaperone machinery. *Exp Biol Med (Maywood)* 228:111–133
2. Kamal A, Thao L, Sensintaffar J, Zhang L, Boehm MF, Fritz LC, Burrows FJ (2003) A high-affinity conformation of Hsp90 confers tumour selectivity on Hsp90 inhibitors. *Nature* 425:407–410
3. BeBoer C, Dietz A (1976) The description and antibiotic production of *Streptomyces hygroscopicus* var. *Geldanus*. *J Antibiotics (Tokyo)* 29:1182–1188
4. Whitesell L, Mimnaugh EG, De Costa B, Myers CE, Neckers LM (1994) Inhibition of heat shock protein HSP90-pp60v-src heteroprotein complex formation by benzoquinone ansamycins: essential role for stress proteins in oncogenic transformation. *Proc Natl Acad Sci USA* 91:8324–8328
5. Dutta R, Inouye M (2000) GHKL, an emergent ATPase/kinase superfamily. *Trends Biochem Sci* 25:24–28
6. Pacey S, Banerji U, Judson I, Workman P (2006) Hsp90 inhibitors in the clinic. *Handbook Exp Pharmacol* 172:331–358
7. Egorin MJ, Lagattuta TF, Hamburger DR, Covey JM, White KD, Musser SM, Eiseman JL (2002) Pharmacokinetics, tissue distribution, and metabolism of 17-(dimethylaminoethylamino)-17-demethoxygeldanamycin (NSC 707545) in CD2F1 mice and Fischer 344 rats. *Cancer Chemother Pharmacol* 49:7–19
8. Eiseman JL, Lan J, Lagattuta TF, Hamburger DR, Joseph E, Covey JM, Egorin MJ (2005) Pharmacokinetics and pharmacodynamics of 17-demethoxy 17-[(2-dimethylamino)ethyl]amino]geldanamycin (17DMAG, NSC 707545) in C.B-17 SCID mice bearing MDA-MB-231 human breast cancer xenografts. *Cancer Chemother Pharmacol* 55:21–32
9. Hollingshead M, Alley M, Burger AM, Borgel S, Pacula-Cox C, Fiebig HH, Sausville EA (2005) In vivo antitumor efficacy of 17-DMAG (17-dimethylaminoethylamino-17-demethoxygeldanamycin hydrochloride), a water-soluble geldanamycin derivative. *Cancer Chemother Pharmacol* 56:115–125
10. Glaze ER, Lambert AL, Smith AC, Page JG, Johnson WD, McCormick DL, Brown AP, Levine BS, Covey JM, Egorin MJ, Eiseman JL, Holleran JL, Sausville EA, Tomaszewski JE (2005) Preclinical toxicity of a geldanamycin analog, 17-(dimethylaminoethylamino)-17-demethoxygeldanamycin (17-DMAG), in rats and dogs: potential clinical relevance. *Cancer Chemother Pharmacol* 56:637–647
11. Shadad FN, Ramanathan RK (2006) 17-dimethylaminoethylamino-17-demethoxygeldanamycin in patients with advanced-stage solid tumors and lymphoma: a phase I study. *Clin Lymphoma Myeloma* 6:500–501
12. Zhang L, Fan J, Vu K, Hong K, Le Brazidec JY, Shi J, Biamonte M, Busch DJ, Lough RE, Grecko R, Ran Y, Sensintaffar JL, Kamal A, Lundgren K, Burrows FJ, Mansfield R, Timony GA, Ulm EH, Kasibhatla SR, Boehm MF (2006) 7'-substituted

benzothiazolothio- and pyridothiazolothio-purines as potent heat shock protein 90 inhibitors. *J Med Chem* 49:5352–5362

- 13. Parkin DM, Bray F (2006) Chapter 2: The burden of HPV-related cancers. *Vaccine* 24(Suppl 3):S11–S25
- 14. Walboomers JM, Jacobs MV, Manos MM, Bosch FX, Kummer JA, Shah KV, Snijders PJ, Peto J, Meijer CJ, Munoz N (1999) Human papillomavirus is a necessary cause of invasive cervical cancer worldwide. *J Pathol* 189:12–19
- 15. Soutter WP, Sasieni P, Panoskaltsis T (2006) Long-term risk of invasive cervical cancer after treatment of squamous cervical intraepithelial neoplasia. *Int J Cancer* 118:2048–2055
- 16. Yuan C, Wang P, Lai C, Tsu E, Yen M, Ng H (1999) Recurrence and survival analyses of 1,115 cervical cancer patients treated with radical hysterectomy. *Gynecol Obstet Invest* 47:127–132
- 17. Whitesell L, Lindquist SL (2005) HSP90 and the chaperoning of cancer. *Nat Rev Cancer* 5: 761–772
- 18. Bagatell R, Paine-Murrieta GD, Taylor CW, Pulcini EJ, Akinaga S, Benjamin IJ, Whitesell L (2000) Induction of a heat shock factor 1-dependent stress response alters the cytotoxic activity of hsp90-binding agents. *Clin Cancer Res* 6:3312–3318
- 19. Guo F, Rocha K, Bali P, Pranpat M, Fiskus W, Boyapalle S, Kumaraswamy S, Balasis M, Greedy B, Armitage ES, Lawrence N, Bhalla K (2005) Abrogation of heat shock protein 70 induction as a strategy to increase antileukemia activity of heat shock protein 90 inhibitor 17-allylamino-demethoxy geldanamycin. *Cancer Res* 65:10536–10544
- 20. McCollum AK, Teneyck CJ, Sauer BM, Toft DO, Erlichman C (2006) Up-regulation of heat shock protein 27 induces resistance to 17-allylamino-demethoxygeldanamycin through a glutathione-mediated mechanism. *Cancer Res* 66:10967–10975
- 21. Schwock J, Geddie WR, Hedley DW (2005) Analysis of hypoxia-inducible factor-1alpha accumulation and cell cycle in geldanamycin-treated human cervical carcinoma cells by laser scanning cytometry. *Cytometry A* 68:59–70
- 22. Pham NA, Gal MR, Bagshaw RD, Mohr AJ, Chue B, Richardson T, Callahan JW (2005) A comparative study of cytoplasmic granules imaged by the real-time microscope, Nile Red and Filipin in fibroblasts from patients with lipid storage diseases. *J Inherit Metab Dis* 28:991–1004
- 23. Xie XY, Robb D, Chow S, Hedley DW (1995) Discordant P-glycoprotein antigen expression and transport function in acute myeloid leukemia. *Leukemia* 9:1882–1887
- 24. Burrows F, Zhang H, Kamal A (2004) Hsp90 activation and cell cycle regulation. *Cell Cycle*, 3:1530–1536
- 25. de Cacer G (2004) Heat shock protein 90 regulates the metaphase–anaphase transition in a polo-like kinase-dependent manner. *Cancer Res* 64:5106–5112
- 26. Okumura E, Fukuhara T, Yoshida H, Hanada Si S, Kozutsumi R, Mori M, Tachibana K, Kishimoto T (2002) Akt inhibits Myt1 in the signalling pathway that leads to meiotic G2/M-phase transition. *Nat Cell Biol* 4:111–116
- 27. Ibrahim NO, Hahn T, Franke C, Stiehl DP, Wirthner R, Wenger RH, Katschinski DM (2005) Induction of the hypoxia-inducible factor system by low levels of heat shock protein 90 inhibitors. *Cancer Res* 65:11094–11100
- 28. Hockel M, Dornhofer N (2005) The hydra phenomenon of cancer: why tumors recur locally after microscopically complete resection. *Cancer Res* 65:2997–3002
- 29. Castle PE, Ashfaq R, Ansari F, Muller CY (2005) Immunohistochemical evaluation of heat shock proteins in normal and preinvasive lesions of the cervix. *Cancer Lett* 229:245–252
- 30. Nomura M, Nomura N, Newcomb EW, Lukyanov Y, Tamasdan C, Zagzag D (2004) Geldanamycin induces mitotic catastrophe and subsequent apoptosis in human glioma cells. *J Cell Physiol* 201:374–384
- 31. Basto R, Gergely F, Draviam VM, Ohkura H, Liley K, Raff JW (2007) Hsp90 is required to localise cyclin B and Msps/ch-TOG to the mitotic spindle in *Drosophila* and humans. *J Cell Sci* 120:1278–1287
- 32. Franke TF, Hornik CP, Segev L, Shostak GA, Sugimoto C (2003) PI3K/Akt and apoptosis: size matters. *Oncogene* 22:8983–8998
- 33. Sato S, Fujita N, Tsuruo T (2000) Modulation of Akt kinase activity by binding to Hsp90. *Proc Natl Acad Sci USA* 97:10832–10837
- 34. Meares GP, Zmijewska AA, Jope RS (2004) Heat shock protein-90 dampens and directs signaling stimulated by insulin-like growth factor-1 and insulin. *FEBS Lett* 574:181–186
- 35. Sanderson S, Valenti M, Gowan S, Patterson L, Ahmad Z, Workman P, Eccles SA (2006) Benzoquinone ansamycin heat shock protein 90 inhibitors modulate multiple functions required for tumor angiogenesis. *Mol Cancer Ther* 5:522–532
- 36. Bisht KS, Bradbury CM, Mattson D, Kaushal A, Sowers A, Markovina S, Ortiz KL, Sieck LK, Isaacs JS, Brechbill MW, Mitchell JB, Neckers LM, Gius D (2003) Geldanamycin and 17-allylamino-17-demethoxygeldanamycin potentiate the in vitro and in vivo radiation response of cervical tumor cells via the heat shock protein 90-mediated intracellular signaling and cytotoxicity. *Cancer Res* 63:8984–8995
- 37. Dote H, Burgan WE, Camphausen K, Tofilon PJ (2006) Inhibition of hsp90 compromises the DNA damage response to radiation. *Cancer Res* 66:9211–9220
- 38. Sharp S, Workman P (2006) Inhibitors of the HSP90 molecular chaperone: current status. *Adv Cancer Res* 95:323–348
- 39. Chaudhury S, Welch TR, Blagg BS (2006) Hsp90 as a target for drug development. *ChemMedChem* 1:1331–1340